Virology 531 (2019) 269–279

Contents lists available at ScienceDirect

Virology

journal homepage: www.elsevier.com/locate/virology

Sumoylation of nucleoprotein (NP) mediated by activation of NADPH oxidase complex is a consequence of oxidative cellular stress during infection by Infectious salmon anemia (ISA) virus necessary to viral progeny

Fernanda Fredericksen, Melina Villalba, Nicolas Maldonado, Gardenia Payne, Francisco Torres, Víctor H. Olavarría*

Facultad de Ciencias, Instituto de Bioquímica y Microbiología, Universidad Austral de Chile, Campus Isla Teja S/N, Valdivia, Chile

ARTICLE INFO

Keywords:
SUMOylation
ISA virus
Maqui
NADPH oxidase complex
ROS
NP

ABSTRACT

The study evaluated the effects of nucleoprotein viral and the infectious virus in SHK-1 cells. The results show a strong respiratory burst activation and the induction of p47phox, SOD, GLURED, and apoptotic genes. Additionally, the cells alter the profile of SUMOylated proteins by the effect of transfection and infection experiments. In silico analyses show a set of structural motifs in NP susceptible of post-translational modification by the SUMO protein. Interestingly, the inhibition of the NADPH oxidase complex blocked the production of reactive oxygen species and the high level of cellular ROS due to the nucleoprotein and the ISAv. At the same time, the blocking of the p38MAPK signaling pathway and the use of Aristotelia chilensis, decreased viral progeny production. These results suggest that the NP triggers a strong production of ROS and modifying the post-translational profile mediated by SUMO-2/3, a phenomenon that favors the production of new virions.

1. Introduction

The infectious salmon anemia (ISA) virus causes high economic losses in the salmon industry in Chile and also the rest of the world (Kibenge et al., 2006). ISAv has tropism for Atlantic salmon (*Salmo salar*), however, it can be detected in other fish, a phenomenon that explains the tenacity of this pathogen in the salmon industry. The virus replicates with a cytopathic effect (CPE) particularly by apoptosis activation (Bouchard et al., 1999; Kibenge et al., 2000; Olavarria et al., 2015a). However, there is currently no information available on the cellular aspects behind the activation of apoptosis in cells of infected fish and that are not necessarily involved in apoptosis. Paradoxically, under conditions of cell death, there is a strong increase in the viral progeny. Although this is a common phenomenon in viral infections, the question remains: what induces cell death? And how does the cell death favors the formation of new infectious virions?

Recently, we found a set of biochemical processes that favor cell damage and/or death as a consequence of viral infection by ISAv, including powerful oxidative stress, which as a whole could begin to answer the first question. (Olavarría et al., 2015b). In this regard, we confirmed that ISAv is able to activate the NADPH oxidase complex, and particularly the p47phox subunit, through the p38 MAPK protein in salmonids, a phenomenon that finally leads to cell death as a result of substantial oxidative imbalance (Olavarría et al., 2015a; Olavarría et al., 2015b). Additionally, a set of experiments demonstrated that ISAv infection strongly decreases the expression of transcripts involved in the synthesis of enzymes able to detoxify oxygen radicals in infected cells, limiting the antioxidant capacity of the infected cell and favoring the apoptosis (Schiøtz et al., 2008). Although the alteration of cellular redox equilibrium irreversibly results in the death of the cell, a set of biochemical processes that precede this consequence have not been analyzed in the ISAv model, and apparently could be beneficial for the formation of new virions.

During oxidative stress, different changes occur in many biological processes, one of them being the SUMOylation of proteins. Interestingly, previous studies have consistently demonstrated that SUMOylation regulates oxidative intracellular stress (Chen et al., 2013; Dangoumau et al., 2013). In fact, variations in oxidative stress can increase the global profile of proteins associated with post-translational modification like SUMO (Manza et al., 2004). For example, modification of SUMO/deSUMOylation balance toward deSUMOylation could be triggered by the cell to re-equilibrate its oxidative homeostasis.

From a molecular point view, post-translational attachment of SUMO (small ubiquitin-like modifier) to the lysine residue(s) of a target

* Corresponding author.
E-mail address: volavarria@uach.cl (V.H. Olavarría).

https://doi.org/10.1016/j.virol.2019.03.012
Received 29 January 2019; Received in revised form 19 March 2019; Accepted 19 March 2019
Available online 20 March 2019
0042-6822/

protein (defined as sumoylation) is a conserved regulatory mechanism (Yang et al., 2013). Firstly, SUMO needs to be hydrolyzed by a SENP (SUMO-specific protease) to expose its C-terminal diglycine motif, a prerequisite for its covalent conjugation. Then, the general process involves a SUMO-activating enzyme (E1, Uba2/Aos1), a single SUMO-conjugating enzyme (E2, Ubc9), and a SUMO-E3 ligase (such as the PIAS family or RanBP2) (Yeh, 2009). Recent studies revealed that SUMOylation regulates cell viability through repressing intracellular ROS generation (Shrivastava et al., 2010). In this context, it has been described that oxidative stress induces a rapid deSUMOylation of several transcription factors including AP-1, c-Fos, and c-Jun among others, causing stimulation of their activity like transcription factors (Bossis et al., 2005; Muller et al., 2000). On the other hand, this set of post-translational modifications is key to the fate of various viral and cellular components in a cellular scenario with strong oxidative activity (Meulmeester and Melchior, 2008). Indeed, during the course of biosynthesis of viral components, various structures of the virus trigger very specific processes within the cell. For example, HCV nucleocapsid protein induces reactive oxygen species (ROS) production in tissue cultures and animal models (Korenaga et al., 2005). However the mechanism(s) by which the core protein induces ROS production are largely unknown, aspect also unidentified in our model of infection by the ISA virus. Tax is another interesting example in which a single viral protein is capable of strongly inducing the production of ROS in the transfected cell (Takahashi et al., 2013) and interestingly, in this cellular context, an efficient formation and maturation of new virions are achieved. On the contrary, the use of blocking molecules of ROS production, like a 2,4-dichlorophenoxyacetic acid (2,4-D), inhibit virus replication in the early stage of influenza virus infection without direct interaction with virus particles. This result is basically achieved through the inhibition of several cellular processes, specifically acidic vesicular formation but mainly the reactive oxygen species production (Enkhtaivan et al., 2017). Therefore, in the context of viral infection, the increase in ROS is related to two opposite processes: the death of the infected cell and formation of a new virus. Therefore, a diametrically opposite result could be obtained by evaluating the use of molecules or compounds with antioxidant activity.

The maqui (*Aristotelia chilensis*) is a native Chilean shrub with anti-inflammatory effects, analgesic properties, antimicrobial activity, and powerful properties against oxidative damage (He et al., 1997; Miranda-Rottmann et al., 2002; Céspedes et al., 2010). Anthocyanins represent water-soluble flavonoid species, and specifically, the delphinidins represent the most potent antioxidant species, with maqui berry being the richest known natural source of this compound (Watson and Schönlau, 2015).

Therefore, the purpose of this study was to evaluate the effect of ISA virus nucleoprotein on the level of ROS production and post-translational modifications in the cell transfected. Changes in the profile expression of SUMOylation, and molecular markers involved in oxidative stress and apoptosis cellular were established through RT-qPCR and Western blot. Additionally, the oxidative stress detection, allowed us to quantify the level of cellular ROS and its relationship with viral production of ISAv in presence of pharmacological inhibitors of the NADPH oxidase complex, p38MAPK and the co-incubation with maqui berry.

2. Materials and methods

2.1. Cell lines and treatments

Monolayer cultures of Atlantic salmon head kidney (SHK-1) were grown in tightly sealed cell-culture flasks (175 cm^2; Sarstedt Inc., Germany) at 16–18 °C and in 20 ml of E-MEM or L-15 (Gibco, USA) supplemented with 2 mm L-glutamine, 0.1 mm non-essential amino acids, 10 mm 4-(2-hydroxyethyl)-1-piperazineethanesulfonic acid (pH 7.0), 1 mg sodium bicarbonate ml^{-1}, 20 µg gentamicin ml^{-1} (Gibco), and 10% fetal bovine serum (Hyclone, GE Healthcare Life Sciences, USA). The applied kinetic transfection considered 8, 16, and 24 h. Parallel experiments included co-stimulation with 100 µM of H_2O_2 (Merck). In some experiments, cells were pretreated for 1 h with 10 µM of SB203580 (p38 MAPK inhibitor), 10 µM of apocynin (NADPH oxidase inhibitor) (all from Sigma-Aldrich) (Olavarría et al., 2010a; Olavarría et al., 2010b) or 1 µM of vitamin C (Leal et al., 2017). A total aqueous extract was prepared from 100 µg of ground and dehydrated *A. chilensis* (Bioherbalis Ltda.), resuspended in 1 ml of PBS. The final solution was used at a concentration of 2% v/v. Under all experimental culture conditions, cell viability was > 95%. For each sampling timepoint, mRNA or protein was extracted and analyzed.

2.2. Viral propagation

A SHK-1 cell line was prepared in a minimum essential growth medium (MEM) at a concentration of 4×10^8 cells/l. These cultures were inoculated with ISAv (designation ISAV-Austral D08I1055-1) at a concentration of 10^6 and a 50% tissue culture infective dose ($TCID_{50}$)/ml at a ratio of 1 ml of virus per 50 ml of cell suspension. Inoculated cells were seeded into a 150 cm^2 tissue culture flask and incubated for 24 h. ISAv-infected SHK-1 cells (0–96 h) were then frozen/thawed twice, harvested, and pelleted by centrifugation at 3000 × *g* for 10 min. The supernatant containing the propagated virus was titrated and quantified by RT-qPCR in the viral experiments (Snow et al., 2006). The virus used in this study underwent 12 in vitro cell culture passages.

2.3. Transfection of nucleoprotein

SHK-1 cells were seeded in 12-well plates and maintained in a 10% L-15 culture medium of fetal bovine serum (SBF) and 1% antibiotic (penicillin/streptomycin) incubated at 16 °C. Cell lines were incubated 24 h before transfection until reaching an approximate confluence of 80%. The cells were transfected with the plasmid pGFP-N1-NP (SHK-1 1000 ng cells) using Lipofectamine 2000 (Invitrogen). Opti-MEM® (Invitrogen) was used for the dilution of Lipofectamine 2000 and pGFP-N1-NP following the manufacturer's instructions. Subsequently, the mixture of both dilutions was made and incubated at room temperature for 20 min to allow forming the Lipofectamine-DNA complexes. The Lipofectamine-DNA complex was adhered by dripping to the wells containing the cells and these were allowed to stand for 1 h, afterwards the different treatments were carried out adding H_2O_2, Apocynin, vitamin c, SB203085 or maqui to finally incubate the cells in their respective growth environments for specific periods. Once the incubation time was over, the medium was removed and the various experiments were carried out.

2.4. Gene expression analysis

To obtain cDNA, total RNA was first extracted from cell pellets with the TRIzol reagent (Invitrogen, USA) following the manufacturer's instructions, and then treated with DNase I, Amplification grade (1 U/mg RNA; Invitrogen). First-strand cDNA was synthesized from total RNA (1 µg) using the SuperScript III RNase H Reverse Transcriptase kit (Invitrogen) with the oligo-dT18 primer at 50 °C for 50 min. Real-time PCR analysis was performed with an ABI PRISM 7500 instrument using the SYBR Green PCR Core Reagents (both from Applied Biosystems, USA). Reaction mixtures were incubated for 10 min at 95 °C, followed by 40 cycles of 15 s at 95 °C and 1 min at 60 °C, and, finally, 15 s at 95 °C, 1 min at 60 °C, and 15 s at 95 °C. For each mRNA, gene expression was normalized to the ribosomal protein S18 (rps18) (Olavarría et al., 2010a; Olavarría et al., 2010b) content in each sample using the comparative Ct method. The primers used for the cellular markers are listed in Table 1. In all cases, each PCR was performed with triplicate samples and was repeated with at least three independent samples.

Table 1
List of primers used in RT-qPCR analysis of immune markers.

Gene	N° Accesion	F	R	bp
p47 phox	FJ594435.1	5-GAGGAGCCTGAAGAAGCTGA-3	5-TCCAGCAGCTTGTGAATGAC-3	134
Bad	BT060150.1	5-TCTACTCCGAGTCCCAGGTG-3	5-ATTTCTTTGCAGCCCACAGT-3	156
Bcl-Xl	NM 001141086	5-GGACTACCCCTTCAACCACA-3	5-GACTCGTCCCGTTGACGTAT-3	107
SOD	NM 001123587.1	5-GGAGACAACGAGGAGAGTCG-3	5-GGTAGAGTTCGGGGGTAAGC-3	164
GLURED	BT045539.1	5-TTCCCACGGTAGTTTTCAGC-3	5-TGCACTGAGTCTTCCTGGTG-3	153
β-Actin	NM 001123525.1	5-ACTGGGACGACATGGAGAAG-3	5-GGGGTGTTGAAGGTCTCAAA-3	157
SUMO 1	NM_001139689.1	5-GGTCAGGACAACAGCGAAAT-3	5-CCTCATCTTCCATTCCAAGC-3	175
SUMO 2/3	NM_001141192.2	5-ATCAACGAGACCGACACACC-3	5-GGAGACTCAGAGGGGTCCAT-3	136
Ubc 9	BT125220.1	5-CATTTGGTTTTGTCGCTGTG-3	5-GGTGGCTCAAACTTGCATTT-3	178
SAE 1	NM_001146514.1	5-GGAAGAAGCGGCTCAGTATG-3	5-TCCTCTGTCACCTGTTCGTG-3	183
SAE 2	NM_001141649.1	5-TGCGCATGCATATCTTTAGC-3	5-CTGCTCCACATCTCCAGACA-3	155

2.5. Immunoprecipitation

SHK-1 cells were lysed in ice-cold NP-40 lysis buffer containing 1% Nonidet P-40, 25 mM Tris-–HCl (pH 7.5), 150 mM sodium chloride, 1 mM EDTA, 5 mM sodium fluoride, 1 mM sodium orthovanadate, 1 mM leupeptin, and 1 mM phenylmethylsulfonyl fluoride. Briefly, cell lysates (500–800 μg of protein determined with the BCA protein assay kit from Pierce) were incubated with the anti-p47phox for 4 h. Cell lysates were then mixed with protein A/G-agarose beads and rotated for 1 h at 4 °C. After the beads were washed three times with ice-cold NP-40 lysis buffer, the precipitated proteins were boiled for 5 min and eluted with sodium dodecyl sulfate-polyacrylamide gel electrophoresis (SDS–PAGE) sample buffer. Immunoprecipitated proteins were resolved in SDS-PAGE and transferred onto nitrocellulose membranes (BioRad).

2.6. Western blotting

Western blot analysis was carried out following a standard protocol (Sambrook et al., 1989). A BCA Protein Assay Kit (Pierce™, Thermo Scientific, USA) was used to determine the cellular extract protein concentrations. Equal amounts of protein were loaded onto polyacrylamide gels, electrophoresed, and transferred onto nitrocellulose membranes (Schleicher & Schuell, USA). After transfer, the membranes were blocked overnight in 5% dry milk and probed for 1 h with anti-anti-SUMO1 (1:2500, #sc-6375, Santa Cruz Biotechnology, USA), or anti-SUMO 2/3 (1:4000, #sc-393144, Santa Cruz Biotechnology, USA), anti-p47phox (1:1000, #sc-14015; Santa Cruz Biotechnology), anti-phospho-Ser (1:2000, #2261, Cell Signaling), anti-nucleoprotein (ANGO) antibodies. Subsequently, the membranes were probed for 1 h with an HRP-coupled secondary antibody (1:5000) (Sigma-Aldrich, USA). The reactive bands were visualized with an enhanced chemiluminescence detection system (Amersham Pharmacia Biotech), following manufacturer instructions. Signal intensity was measured with the ImageJ digital imaging system.

2.7. In silico analysis

The MEME/MAST system version 3 (http://meme.nbcr.net/meme/cgi-bin/mast.cgi), GPS-SUMO (http://sumosp.biocuckoo.org/online.php), phosphor-motif (http://kinasephos.mbc.nctu.edu.tw/) and Chimera 1.8 (https://www.cgl.ucsf.edu/chimera/download.html) for motif discovery and search were used to predict conserved sequence domain in the NP.

2.8. Oxidative stress evaluation

SHK-1 cells were seeded in Lab-Tek ™ Chamber Slides (Nunc ™, Thermo Scientific) at a confluence of 80%, maintained in 10% L-15 culture medium of fetal bovine serum (SBF) and 1% antibiotic, and incubated at 16 °C for 24 h prior to transfection. Once the cells were transfected with pGFP-N1-NP and with their respective treatments, oxidative stress was evaluated using the CellROX® probe (Life Technologies) following the manufacturing instructions. Briefly, the probe was added to the SHK-1 cells at a final concentration of 5 μM. It was incubated for 30 min at 37 °C to subsequently remove the medium and washed 3 times with PBS 1 × . Then, the cells were fixed with 3.7% paraformaldehyde for 15 min, permeabilized with 0.1% TritonX-100 for 10 min and incubated with DAPI 1:10000 for the visualization of nuclei. Finally, a mounting medium was added and the Chamber Slide was covered with a coverslip. For the visualization of oxidative stress, the OLYMPUS IX71 epifluorescence microscope (Olympus) was used at a magnification of 100 × .

2.9. Effect antiviral assay

Effect antiviral assay was performed in a confluent monolayer of SHK-1 cells in 96-well plate in duplicate by MTT (3-(4,5-dimethyl thiazol-2yl)-2,5-diphenyl tetrazolium bromide) assay as described by Smee et al. (2003). The monolayer was infected with MOI:5 cell and the virus-infected cells were treated with SB203085, vitamin C, and maqui. Untreated wells of infected cells (virus controls), uninfected cells (cell controls), and drug cytotoxicity controls (cells and drugs only, using the same dilution range for each drug as the test wells) were evaluated (data not shown). At four days post-infection, virus control wells exhibited 100% cytopathology.

2.10. MTT assay

For the MTT assay, the same plates were stained with 10 ml MTT dye (Promega, U.S.A) and the formazan crystals developed were dissolved using SDS solution (sodium dodecyl sulfate) (Promega, USA), and the absorbance was measured at 570 nm in ELISA reader. Mean absorbance values of the duplicates were calculated for cell control and virus in the conditions for each experiment. The absorbance developed in test wells was compared with control wells to calculate the percentage of SHK-1 cell survivability, as a direct measure of cellular toxicity, and indirectly of viral replication.

2.11. Statistical analysis

All data are shown as the mean ± SE. Differences were evaluated using ANOVA followed by the Student's *t*-test. Statistical significance was defined as $P < 0.05$.

3. Results

3.1. Molecular characteristic of NP

The phylogenetic analysis of 33 amino acid sequences of NP, shows the high degree of structural conservation among isolates from different latitudes (Fig. 1a). The model NP molecule contains 495 amino and has a high alpha helix structure density (38%), interspersed with beta

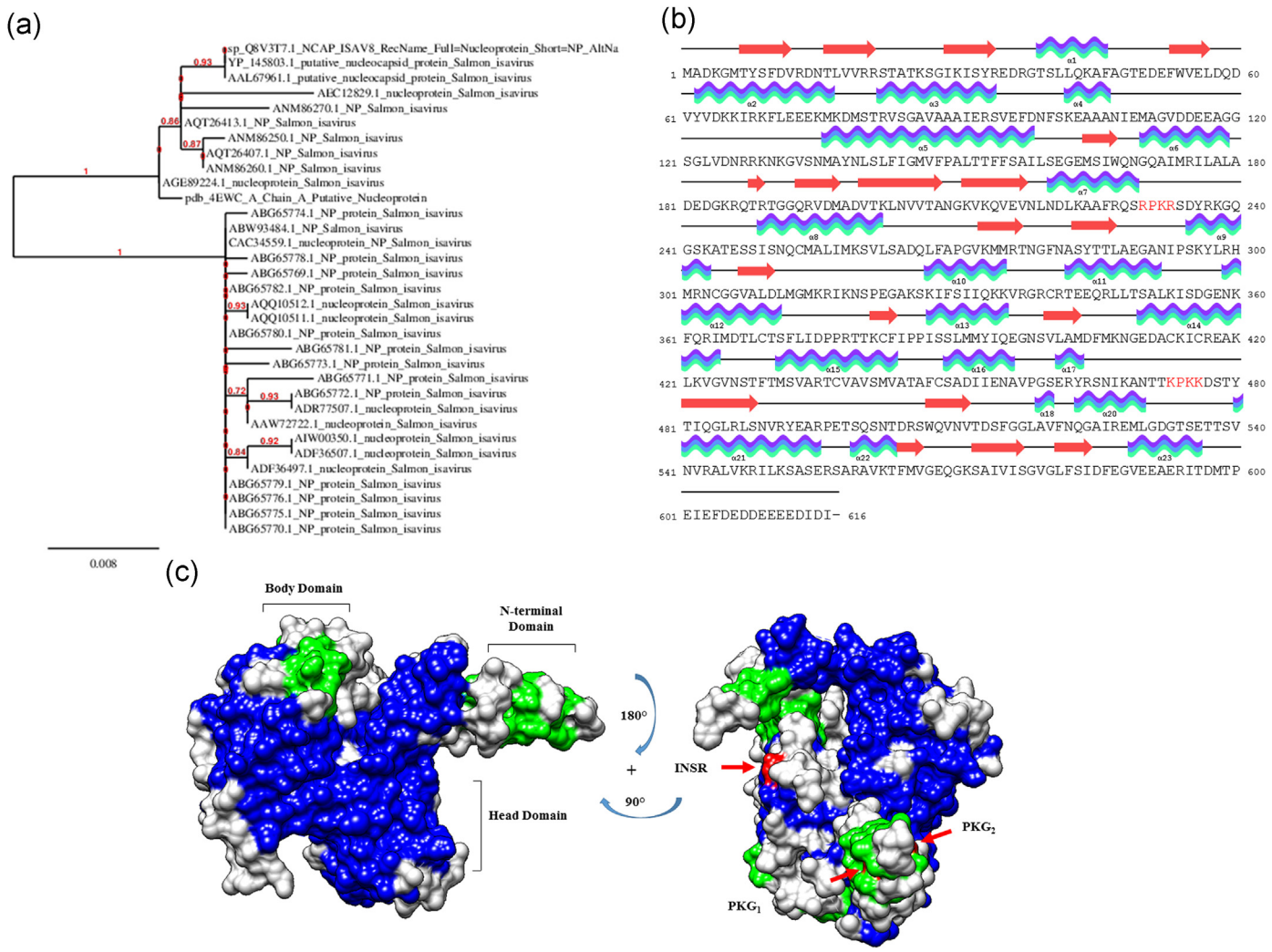

Fig. 1. Molecular characterization of NP. (**a**) Phylogenetic tree showing the genetic relationship between the 33 NP sequences. Sequences were aligned and the phylogenetic tree was generated by using CLUSTAL X. Phylogenetic analysis using Neighbor-Joining bootstrap method (1000 replicates) provided satisfactory bootstrap support. (**b**) ISAv-NP secondary structure assignment. Zig zag structures indicate α-helices and β-strands are represented by arrows. Monopartite nuclear localization signal residues are highlighted in red. The NP sequences from ISAv and the influenza A virus were manually aligned, based on tertiary structures. (**c**) Orthogonal views of an NP dimer. One subunit is colored in blue whereas the other subunit is colored by domains, with gray and green for the N-terminal domain, and red for the potential phosphorylation motif. The structure presents three well-defined regions; Body domain, Head domain and N-terminal domain.

structure folded sheet (11%) (Fig. 1b). This structure can be divided into three domains: an N-terminal domain, a head domain, and a body domain (Fig. 1c). The N-terminal domain contains two potential monopartite nuclear localization signals; ^{230}RPKR^{233} and ^{473}KPKK^{476} (Fig. 1b). From the signaling pathway point of view, NP presents a series of potential protein motifs for cell kinase recognition (Table 2). Of the total of 15 potential amino acid regions, only 3 of them have a moderate-high probability of recognition, in particularly PKG and INSR. Additionally, they are exposed on the surface of the protein. (Fig. 1c, right).

3.2. NP increases the expression/activation of p47phox and ROS production

The nucleoprotein was overexpressed in SHK-1 cells (Fig. 2a), and then, the level of expression of p47phox was determined by RT-qPCR. Interestingly, from 8 h post-transfection, a strong increase in p47phox was observed, which remained at 24 h post-transfection. The same experiment performed in the presence of H_2O_2, increased the expression of p47phox by 230%, however, in the presence of the pharmacological inhibitor apocynin, the level of transcript returned to the basal condition (Fig. 2b). A similar phenomenon was observed at the protein level. The expression level of p47phox is drastically increased by the presence of NP. In fact, it is possible to demonstrate the real effect of the transfected NP protein on the p47phox level, by comparing the signal intensity generated with the GFP transfection (Fig. 2c). Interestingly, the oxidative contribution of H_2O_2 favors the greater expression of p47phox, a phenomenon that tends to decrease due to the effect of the inhibitor of the NADPH oxidase complex. Recently, we demonstrated the ability of the ISA virus to activate the NADPH oxidase complex (Olavarria et al., 2015a; Olavarria et al., 2015b). Therefore, the obvious question was: Will NP alone have an effect on the activation of p47phox? To our surprise, the mere presence of NP stimulates the phosphorylation of p47phox, at similar level of the ISA virus, which is the previous step to the activation of the NADPH oxidase complex. Interestingly, this process was blocked by a pharmacologic inhibitor of p38MAPK (Fig. 2d). In the cellular context, this activation of p47phox resulted in a strong oxidant signal by the CellROX reagent, a fluorogenic probe for measuring oxidative stress in cells, which was more robust in combination with H_2O_2 and a slight decrease in the presence of apocynin (Fig. 2e). Therefore, our results demonstrate that the presence of NP in SHK-1 cells stimulates the production and activation of

Table 2
Potential protein motifs for cell kinase recognition in NP protein.

Localitions (AA)	Phosphorylated Sites	E-value	Catalytic Kinases	Predictive Models
22	VVRRSTATK	41	PKG	
23	VVRRSTATKS	15	PKA	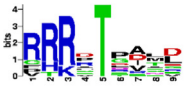
32	GIKISYRED	56	PKG	
62	DQDVYVDKK	34	Syk	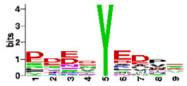
84	STRVSGAVA	20	PKG	
188	GKRQTRTGG	18	PKA	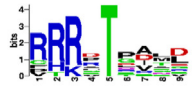
236	KRSDYRKGQ	86	INSR	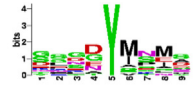
248	ATESSISNQ	35	CKI	
320	RIKNSPEGA	9.6	cdc2	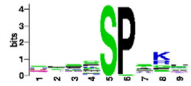
436	GSERYRSNI	97	INSR	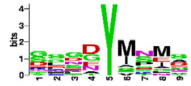
465	ERYRSNIKA	40	PKG	
499	RPETSQSNT	46	ATM	
554	LKSASERSA	7.9	CKII	
599	ITDMTPEIE	6.3	cdc2	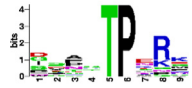
599	ITDMTPEIE	9.6	MAPK	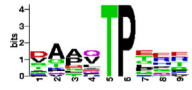

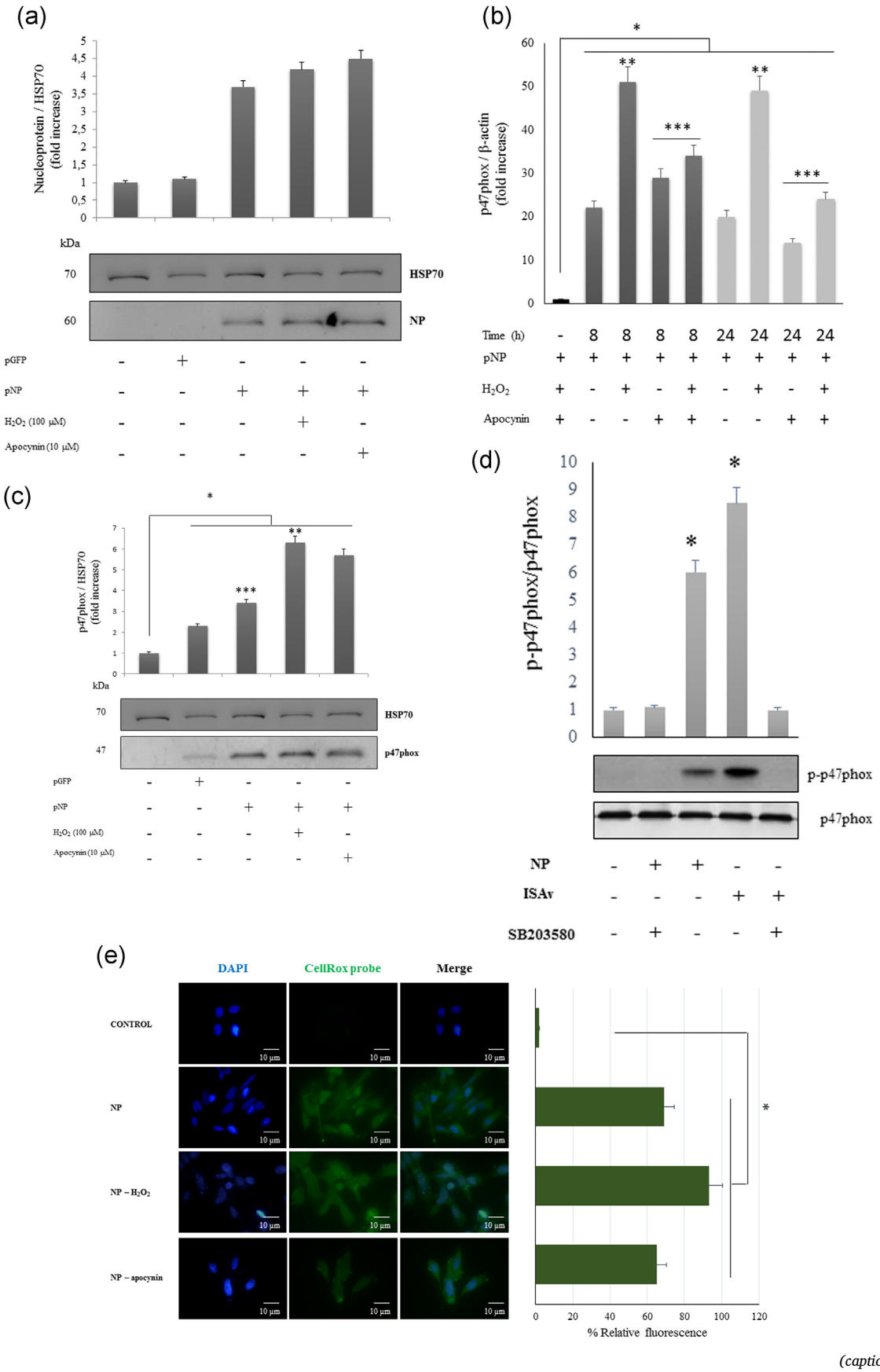

(caption on next page)

Fig. 2. NP increases the ROS production. (**a**) Transfection of cells with pNP, evaluated through Western blot assay. The results show that under evaluated conditions there is no significant effect on the level of NP protein. (**b**) Quantification of p47phox transcript by RT-qPCR in different incubation conditions at 8 and 24 h post-transfection. Each bar represents the mean ± SE of triplicate samples. *P < 0.05 versus untransfected cells. **P < 0.05 versus transfected cells without H_2O_2. ***P < 0.05 versus transfected cells with H_2O_2 and without apocynin. (**c**) Quantification of p47phox by Western blot in different incubation conditions in 24 h, post-transfection. Each bar represents the mean ± SE of triplicate samples. *P < 0.05 versus untransfected cells. **P < 0.05 versus transfected cells without H_2O_2. ***P < 0.05 versus transfected with pGFP. (**d**) Quantification of phospho-p47phox protein by immunoprecipitation and Western blot analyses during transfection with pNP and infection with ISAv (MOI 5) at 8 h in presence or absence of the pharmacological inhibitor of p38MAPK (SB203580). *P < 0.05 versus NP plus SB203580 or ISAv plus SB203580, respectively. (**e**) SHK-1 cells were transfected for 8 h with NP, and the ROS levels of several conditions were determined using a specific fluorescent probe. Each bar represents the mean ± SE of triplicate samples. *P < 0.05 versus untransfected cells. The results are representative of three independent experiments.

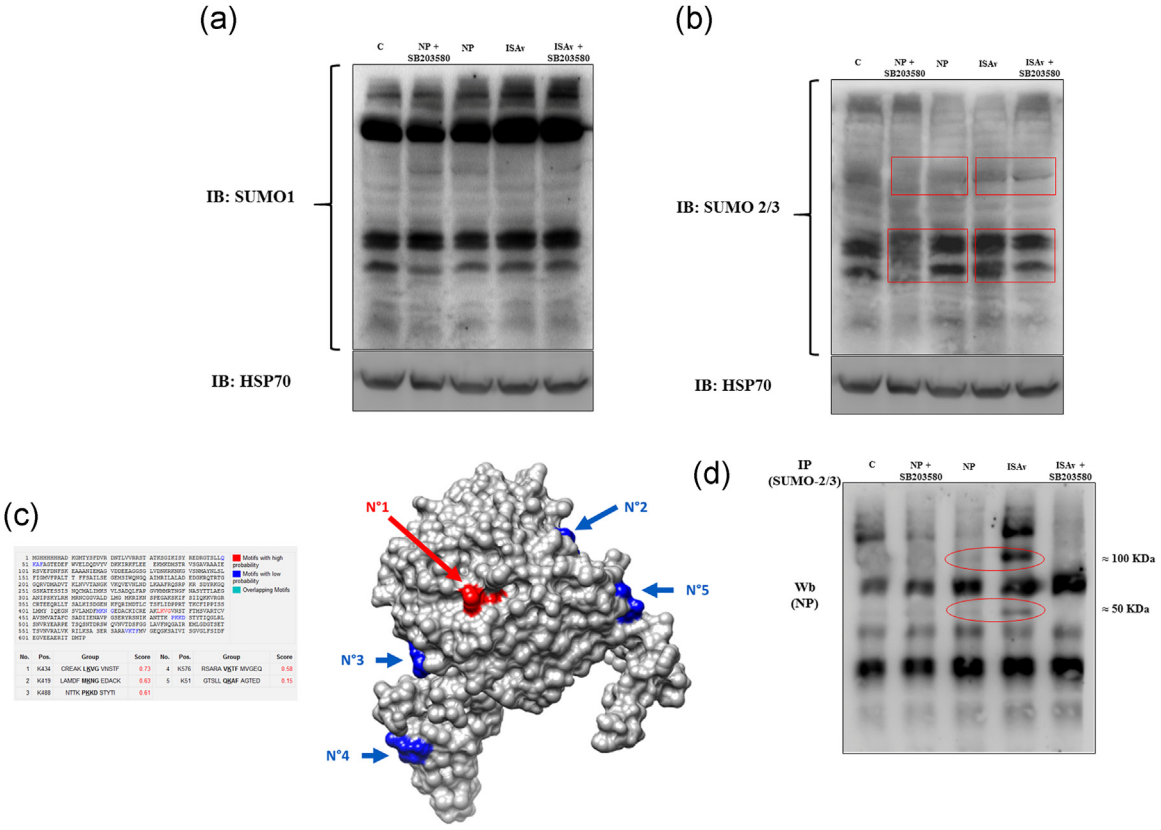

Fig. 3. Effects of viral components in cellular SUMOylation. (a) Western blot analyses during transfection or infection with NP and ISAv, respectively for 8 h. SUMO-1 protein expression profile in presence or absence of pharmacologic inhibitor of p38MAPK (SB203580). Bottom, load control, using HSP70. (**b**) Western blot analyses of SUMO-2/3 protein in similar conditions. (**c**) Analyses of SUMO protein acceptor motifs by GPS-SUMO and Chimera 1.8 tools in NP protein of ISA virus. (**d**) Immunoprecipitation and Western blot analyses of NP protein in transfection or infection experiments in presence or absence of the pharmacological inhibitor of p38MAPK (SB203580). The results are representative of three independent experiments.

p47phox, favoring the assembly of the NADPH oxidase complex and the respiratory burst of the cell.

3.3. NP alters the level of SUMOylated proteins

Our background suggests the potential connection between the ISA virus, oxidative stress and the level of cellular SUMOylation. In order to identify the possible participation of NP in the degree of post-translational modification mediated by SUMO in the SHK-1 cells transfected with NP, a Western blot analyses was performed from cells treated in different conditions. Fig. 3a, shows a similar protein profile of SUMOylation in the SHK-1, mediated by SUMO-1, in all evaluated conditions. However, when the profile of total proteins incorporating SUMO 2/3 was evaluated, it was possible to demonstrate electrophoretic differences both in the cells transfected with NP and in the cells infected with ISAv (Fig. 3b). In fact, when observing the effect of the inhibitor SB303485, it is possible to see a significant decrease of specific signals of SUMO 2/3, result that could suggest a potential connection between p38MAPK, the production of ROS and the modification of the cellular SUMOylation profile (Fig. 3b). The cellular SUMOylation machinery, post-translationally modifies potential substrates that have specific aminoacidic regions. In this sense, another point of interest was to identify potential SUMOylation motifs in the NP protein. Using the GPS-SUMO and Chimera 1.8 tools, we identified 5 potential SUMO protein acceptor motifs. Our analysis identified 1 motif with high probability and 4 aminoacidic motifs with low probability of SUMO-incorporation, however, all these regions were potentially exposed and accessible to the SUMOylation machinery (Fig. 3c). Although the immunoprecipitation assays of SUMO 2/3 demonstrated the incorporation of this isoform of SUMO into the NP protein, in both the transfection and infection experiments the presence of SB203085 blocked this post-translational modification (Fig. 3d). Additionally, when evaluating the incorporation of SUMO-1, its presence in the NP protein was not detected (data not shown). Therefore, this set of experiments demonstrate that both NP and infection with the ISA virus is capable of modifying the degree of SUMOylation in proteins that are acceptors of this post-translational label. Additionally, through RT-qPCR tests, we demonstrated that this process is solely a consequence of

Table 3
Analysis of expression of molecular markers.

p47 phox	t (h)	8	24	48
	Control	1 ×	1 ×	1 ×
	ISAv	22 ×	39 ×	42 ×
	NP	48 ×	45 ×	37 ×
Bad	**t (h)**	**8**	**24**	**48**
	Control	1 ×	1 ×	1 ×
	ISAv	3,5 ×	4,8 ×	5,7 ×
	NP	1,7 ×	1,9 ×	2,1 ×
Bcl-xl	**t (h)**	**8**	**24**	**48**
	Control	1 ×	1 ×	1 ×
	ISAv	2,1 ×	1,7 ×	1,5 ×
	NP	1,5 ×	1,8 ×	1,8 ×
SOD	**t (h)**	**8**	**24**	**48**
	Control	1 ×	1 ×	1 ×
	ISAv	1,7 ×	1,5 ×	1,3 ×
	NP	1,9 ×	1,8 ×	2,1 ×
GLURED	**t (h)**	**8**	**24**	**48**
	Control	1 ×	1 ×	1 ×
	ISAv	2,5 ×	3,2 ×	3,7 ×
	NP	1,7 ×	1,8 ×	1,5 ×
Ubc 9	**t (h)**	**8**	**24**	**48**
	Control	1 ×	1 ×	1,2 ×
	ISAv	1 ×	1,2 ×	0,55 ×
	NP	0,6 ×	0,9 ×	0,85 ×
SUMO 1	**t (h)**	**8**	**24**	**48**
	Control	1 ×	1,1 ×	1,2 ×
	ISAv	0,9 ×	1,2 ×	0,75 ×
	NP	0,7 ×	0,9 ×	0,75 ×
SUMO 2/3	**t (h)**	**8**	**24**	**48**
	Control	0,9 ×	0,9 ×	1,0 ×
	ISAv	1 ×	1,2 ×	0,55 ×
	NP	0,8 ×	0,9 ×	0,8 ×
SAE1	**t (h)**	**8**	**24**	**48**
	Control	1 ×	1 ×	1,0 ×
	ISAv	1,1 ×	1,2 ×	1,1 ×
	NP	0,9 ×	0,9 ×	0,9 ×
SAE 2	**t (h)**	**8**	**24**	**48**
	Control	0,8 ×	0,85 ×	0,9 ×
	ISAv	1 ×	1,2 ×	0,65 ×
	NP	0,6 ×	0,9 ×	0,65 ×

the activation of the cellular SUMOylation machinery and not of a change in the expression of the enzymes involved in the process (Table 3).

3.4. Blockade of ROS production decreases ISA viral progeny

So far, the experiments carried out show that the NP protein and the ISA virus are capable of activating the NADPH oxidase complex through the p38MAPK signaling pathway. The increase of cellular ROS, is closely linked to the activation of the machinery of SUMOylation that modifies the profile of cellular proteins and even of the virus. Therefore, in order to confirm the need for the ISA virus by an apparent strongly oxidizing environment, the production of virions was quantified in the presence of pharmacological inhibitors involved in the activation of the NADPH oxidase complex, p38MAPK, and natural scavengers of oxygen radicals.

When ISA virus infection was challenged with SB203085, there was a decrease of approximately 50% of the viral load at 48 and 96 hpi. The blocking of the NADPH oxidase complex was significantly lower than that achieved by interrupting the activity of p38MAPK (Fig. 4a). On the contrary, the use of vitamin C had no significant effect on viral genome production. However, the effect achieved by the aqueous extract of the maqui on the viral progeny, comparable with SB203085, was unexpected because it practically generated a 50% decrease in ISA virus replication (Fig. 4a). Evidently, in this dichotomy of survival, the effect of each condition was evaluated from the point of view of the infected cell. The results confirm the cellular protective effect, up to 96 h, of both SB203085 and the aqueous extract of maqui (Fig. 4b). Additionally, it was evident a significative modulation of apoptotic and antioxidant markers by the effect of scavengers of oxygen radicals (Table 3). Therefore, these results strongly suggest a diametrically opposite role of oxygen radicals, both for the dead of the cell and the survival ISA virus.

4. Discussion

The Orthomyxoviridae family has been extensively studied due to its wide impact on public health worldwide. Although important discoveries have been made, essential aspects of the infection mechanism of these viruses remain unknown. Clearly, gaining a better understanding of the infection mechanism of ISAv will bring us closer to discovering a therapeutic target or designing an efficient antiviral treatment highly specific to this virus. On the other hand, ISAv is a globally-important pathogen of farmed Atlantic salmon (*Salmo salar*) and is currently listed by the World Organisation for Animal Health (OIE, 2017). Indeed, when ISAv is detected, efficient responses by industry and disease regulatory agencies help to contain viral spread from an index-case farm site to neighboring farm sites (Mardones et al., 2014). The above shows that ISAv is an active pathogen, either as a model to obtain information that can be applied on other Orthomyxoviruses of interest to humans or to improve the knowledge of the infection mechanism of this aquatic pathogen.

A set of preliminary research regarding the NADPH oxidase mechanism in fish, as well as the characterization of oxidative stress mediated by the ISA virus, allowed us to continue exploring in the search for new molecular aspects linked to the infection process (Olavarría et al., 2010a; Olavarría et al., 2010b; Olavarría et al., 2012; Olavarria et al., 2015a; Olavarria et al., 2015b). A key component of our strategy to study ISAv was to understand the role of each of its components separately, and within this context diverse antecedents led us to study the participation of NP as an independent structure in the course of the infection by ISA virus.

The NP is a 56 kDa monomeric basic protein that packages the RNA segments with a periodicity of one protein for each of the 24 bases of RNA, reaching a high concentration in the cell during the stage of viral biosynthesis (Ortega et al., 2000). Currently, the consequence of this abrupt increase of NP in the cell is unknown. It is probable that the nucleoprotein interacts with various cellular switches as a consequence of its structural characteristics (Prokudina et al., 2005; Chou et al., 2012), a phenomenon that could contribute as a whole to the pathogenesis of the ISA virus. In silico analyzes show a series of potential phosphorylation sites by different cellular kinases (Table 1, Fig. 1c), the N-terminal domain has two proteins motif substrates of PKG (cGMP-dependent protein kinase) and INSR (Insulin Receptor). Even though there are currently no studies linking Orthomyxovirus with PKG, this kinase has been shown to phosphorylate NS5 of West Nile virus (WNV), and although PKG is not required for WNV replication, this kinase does make a stable interaction with NS5 (Keating et al., 2013). On the other hand, the insulin receptor (INSR), with tyrosine kinase activity mediates the pleiotropic actions of insulin. In fact, binding of insulin leads to the phosphorylation of several intracellular substrates. In another example, a report shows how the HBV (hepatitis B virus) pre-S2 protein decreases INSR activity in cells infected with the virus, which could represent a mechanism of sequestering a cellular kinase or modulation of a cellular process (Ji et al., 2009).

Currently, our analysis and the few examples of interaction between cellular kinases and viral proteins could preliminarily suggest a post-translational modification of NP or another viral protein by host enzymes. What is the consequence of this? For the moment we do not know, and the possibilities are endless.

Our results show that the increase in NP stimulates both the synthesis and the activation of the p47phox subunit (Fig. 2b, c, and d). A similar phenomenon was observed by the Tat (transactivator of transcription) protein of the HIV virus. Specifically, Tat-induced

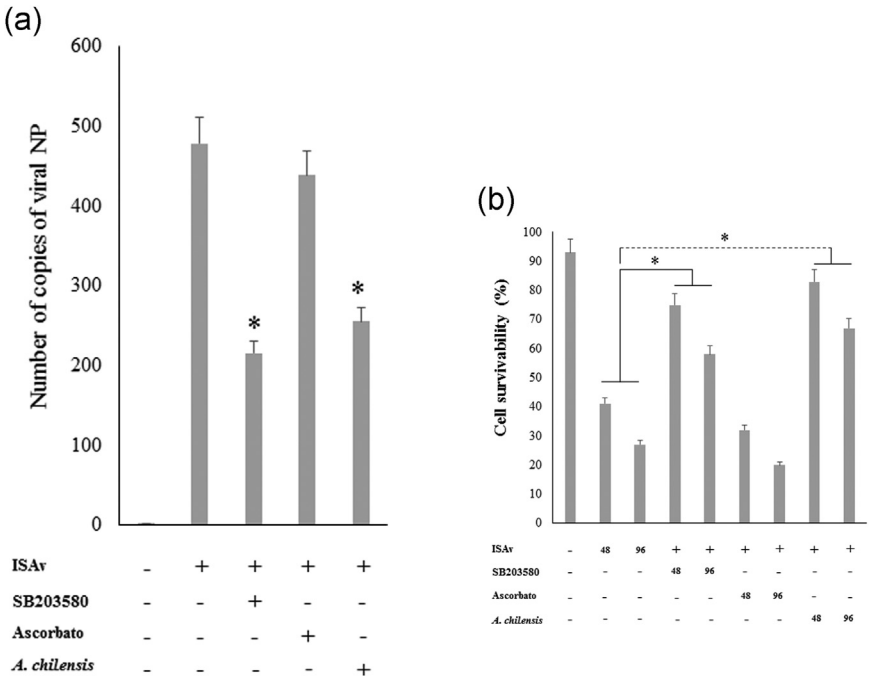

Fig. 4. Blockade of ROS production decreases ISA viral progeny. (**a**) Quantification of NP transcript by RT-qPCR under different infection conditions in 48 h (MOI 5). Each bar represents the mean ± SE of triplicate samples. *P < 0.05 versus cells without SB203580 or *A. chilensis*. (**b**) Determination of cell survival by MTT analysis in presence or absence of pharmacologic inhibitors or free radical scavengers at 48 or 96 h. Each bar represents the mean ± SE of triplicate samples. *P < 0.05 versus cells with virus, without SB203580 or *A. chilensis* at 48 or 96 h, respectively.

expression of NADPH oxidase subunits, such as Nox2, p47phox, and p22phox, additionally trigger the generation of ROS (Youn et al., 2017). It must be noted that both NP and the ISA virus strongly increase the phosphorylation of p47phox, and this results in an increase in cellular ROS (Fig. 2d, e).

Recently, we had shown that the viral particle stimulated the activity of the NADPH oxidase complex, however, it seemed extremely interesting to confirm that the presence of NP in the cell generates a similar result (Olavarría et al., 2015). Apparently, this topic has been described in other Orthomyxoviruses, with which it is possible to identify a pattern of action in this viral family that is related with the generation of viral progeny in a scenario of oxidative stress. Particularly, highly pathogenic H5N1 infection is also related to oxidative stress. Indeed, negative modulation of SOD1 (Cu/Zn superoxide dismutase) by the effect of the virus generates an increase in ROS that allows the replication of the virus (Lin et al., 2016).

The accepted definition of oxidative stress is an imbalance between oxidants and antioxidants when the organism is exposed to adverse stimuli (Sies, 1997). During the accumulation of ROS, the balance between the oxidation system and antioxidant system is broken, resulting in accumulation of oxidation intermediate, tissue damage, inflammation, and apoptosis. Incipient evidence has demonstrated that oxidative stress is an important contributor to infectious diseases such as HBV, HCV, HSV and influenza (Pasquier, 1994; Ha et al., 2010; Gonzalez-Dosal et al., 2011; Mileva, 2016). Apparently, this increase in ROS modulates the participation of different signaling processes that benefit the virus (Fig. 3d, Fig. 4a). Specifically, in this study, we have shown a relationship between the increase in ROS and cellular SUMOylation. In this sense H_2O_2, is known to target several kinases and phosphatases, for example, NADPH oxidase leads to the activation of the kinase EGFR (epidermal growth factor receptor), contrary the same metabolite inactivates IKK (IκB kinase) (Truong and Carroll, 2012; Truong and Carroll, 2013). In another example, H_2O_2 treatment of human endometrial stromal cells activates JNK (c-Jun N-terminal), phosphorylates PIAS1 (Protein Inhibitor of Activated STAT 1). This enhances its SUMO E3 ligase activity and promotes a global increase in protein SUMOylation (Leitao et al., 2011), phenomenon apparently similar to that observed in our study model. Therefore, modification of kinase and phosphatase activities by ROS leads to the remodeling of the phosphorylation state of many proteins and can influence SUMOylation at two levels: Phosphorylation can regulate the activity and/or localization of SUMO enzymes and it can influence target recognition by the machinery. At present, there are not meta-proteomic or metabolomics analyses linked to the infective process by ISAv, therefore, several studies at the meta-transcriptomic level allow us to infer the impact that the virus has on the level of expression of molecular markers as a consequence of the activation or inhibition of different kinases or phosphatases involved in signaling pathways (Dettleff et al., 2017; Valenzuela-Miranda et al., 2015a; Valenzuela-Miranda et al., 2015b; Valenzuela-Miranda et al., 2015a; Valenzuela-Miranda et al., 2015b), although until now no relationship between ISAv, oxidative stress, and SUMOylation has been described.

SUMOylation is considered to be a major regulatory system of protein function that targets many substrates through direct SUMOylation and protein-protein interactions (Wilson, 2012). Viruses have evolved to use the conserved SUMOylation system for their own benefits. Recent advances have suggested that viral proteins work as the targets of the SUMOylation machinery byways of affecting its biological functions (Everett et al., 2013). Additionally, many viral proteins participate in the regulation of host SUMOylation system, even mimicking the related enzymes (Wimmer et al., 2012; Mattoscio et al., 2013).

Therefore, if we consider that during the viral infection, and as a consequence of the strong increase of viral components, there is an alteration of the cellular redox state we must maintain the premise “all cells incubated under a condition of elevated oxidative stress resulted in an increase in the SUMOylation of proteins” (Bossis and Melchior, 2006). Emerging evidence strongly suggests that altering the delicate balance of SUMOylation could be important to the development of many pathologies such as cancer, diabetes, and neurodegenerative diseases, among others (Wang and Banerjee, 2004; Wang et al., 2006). Moreover, SUMOylation could also be involved in the progression of infection in a number of viral models (Lee et al., 2014; Everett et al., 2014; Scherer et al., 2013). Evidently, the contribution of our study is based on the fact that a single protein of the ISA virus is capable of generating the conditions to alter the cellular oxidative balance associated with the post-translational modification mediated by the SUMO protein (Figs. 2d, 3b, 3d). Our results suggest that the imbalance in cellular SUMO activity is a consequence of the redox imbalance of the cell during viral infection, but can also be explained by the high expression of a single protein of the virus.

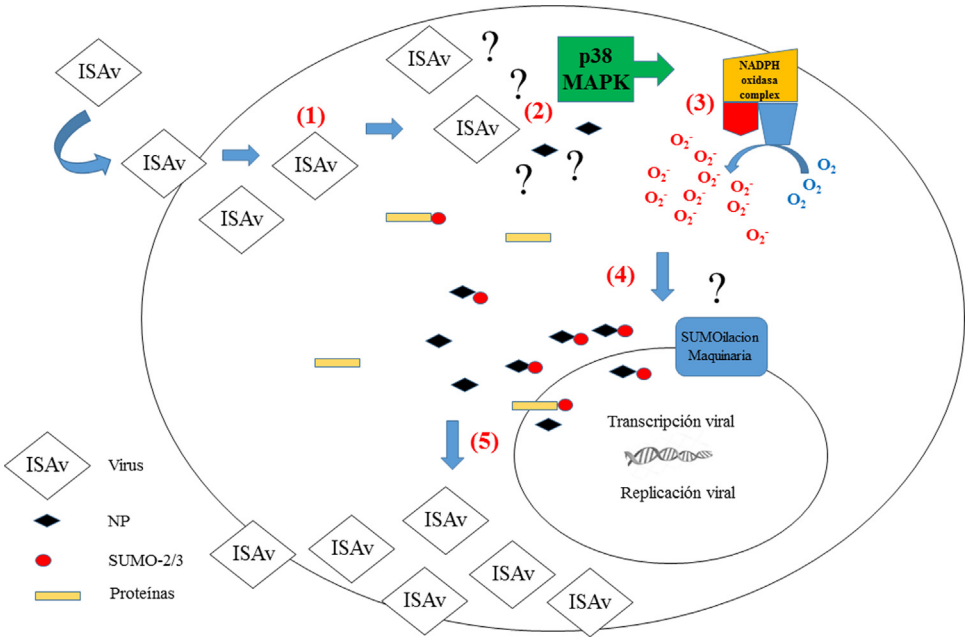

Fig. 5. Summary model of the results. (**1**) The infection of the ISA virus affects diverse cellular processes and we recently showed that it has an effect on the p38MAPK signaling pathway (Olavarria et al., 2015a; Olavarría et al., 2015b). (**2**) During the biosynthesis of viral components, overexpression of the NP protein is able to activate p38MAPK on its own, however, the precise mechanism of this process is unknown. (**3**) The p38MAPK phosphorylates p47phox and the consequent activation of the NADPH oxidase complex increases ROS production. (**4**) The strong and drastic increase of cellular ROS activates the machinery of SUMOylation by an unknown mechanism, without altering the expression of its components. (**5**) Various cellular and viral proteins mainly incorporate SUMO-2/3, biochemical process that favors the generation of new viral progeny. Interestingly, the blockade of stage 2 or 3, results in the reduction of viral particle synthesis and increased survival of the infected cell. On the contrary, the increase of oxygen radicals (H_2O_2) favors the production of virions and less stability of the host.

5. Conclusions

This study demonstrated, for the first time, that NP protein and ISA virus were able to activate the NADPH oxidase complex producing ROS in fish cells. In parallel, the presence of NP and ISAv modulated the expression of apoptotic markers and genes involved in the detoxification of oxygen radicals. The cellular oxidative condition resulted in the incorporation of SUMO 2/3 in host proteins and NP protein, a phenomenon that was partially blocked by the use of the pharmacological inhibitor of p38MAPK and the natural product "maqui". These two protective conditions were able to decrease cell damage because they significantly affected the production of new viral progeny (Fig. 5).

Acknowledgments

This work was supported by Fondecyt (grant N° 11150560), and the Direccion de Investigación y Desarrollo de la Universidad Austral de Chile (DID-UACh), Chile.

References

Bossis, G., Malnou, C.E., Farras, R., Andermarcher, E., Hipskind, R., Rodriguez, M., 2005. Down-regulation of c-Fos/c-Jun AP-1 dimer activity by sumoylation. Mol. Cell. Biol. 25, 6964–6979.
Bossis, G., Melchior, F., 2006. SUMO: regulating the regulator. Cell Div. 29 (1), 13.
Bouchard, D., Keleher, W., Opitz, H.M., Blake, S., Edwards, K.C., Nicholson, B.L., 1999. Isolation of infectious salmon anemia virus (ISAV) from Atlantic salmon in New Brunswick, Canada. Dis. Aquat. Organ 35, 131–137.
Céspedes, C., Valdez-Morales, M., Avila, J., El-Hafidi, M., Alarcón, J., Paredes-López, O., 2010. Phytochemical profile and the antioxidant activity of Chilean wild black-berry fruits, Aristotelia chilensis (Mol) Stuntz (Elaeocarpaceae). Food Chem. 119, 886–895.
Chen, C.H., Chang, C.C., Lee, T.H., Luo, M., Huang, P., Liao, P.H., Wei, S., Li, F.A., Chen, R.H., Zhou, X.Z., Shih, H.M., Lu, K.P., 2013. SENP1 deSUMOylates and regulates Pin1 protein activity and cellular function. Cancer Res. 73, 3951–3962.
Chou, Y.Y., Vafabakhsh, R., Doganay, S., 2012. One influenza virus particle packages eight unique viral RNAs as shown by FISH analysis. Proc. Natl. Acad. Sci. USA 109, 9101–9106.
Dangoumau, A., Veyrat-Durebex, C., Blasco, H., Praline, J., Corcia, P., Andres, C.R., Vourc'h, P., 2013. Protein SUMOylation, an emerging pathway in amyotrophic lateral sclerosis. Int. J. Neurosci. 123, 366–374.
Dettleff, P., Moen, T., Santi, N., Martinez, V., 2017. Transcriptomic analysis of spleen infected with infectious salmon anemia virus reveals distinct pattern of viral replication on resistant and susceptible Atlantic salmon (Salmo salar). Fish. Shellfish Immunol. 61, 187–193.
Enkhtaivan, G., Muthuraman, P., Kim, D.H., 2017. Inhibitory effect of 2,4-dichlorophenoxyacetic acid on ROS, autophagy formation, and mRNA replication for influenza virus infection. J. Mol. Recognit. 30.
Everett, R.D., Boutell, C., Hale, B.G., 2013. Interplay between viruses and host sumoylation pathways. Nat. Rev. Microbiol. 11, 400–411.
Everett, R.D., Boutell, C., Pheasant, K., Cuchet-Lourenço, D., Orr, A., 2014. Sequences related to SUMO interaction motifs in herpes simplex virus 1 protein ICP0 act cooperatively to stimulate virus infection. J. Virol. 88, 2763–2774.
Gonzalez-Dosal, R., Horan, K.A., Rahbek, S.H., Ichijo, H., Chen, Z.J., Mieyal, J.J., 2011. HSV infection induces production of ROS, which potentiate signaling from pattern recognition receptors: role for S-glutathionylation of TRAF3 and 6. PLoS Pathog. 7, e1002250.
Ha, H.L., Shin, H.J., Feitelson, M.A., Yu, D.Y., 2010. Oxidative stress and antioxidants in hepatic pathogenesis. World J. Gastroenterol. 16, 6035–6043.
He, K., Valcic, S., Timmermann, B.N., Montenegro, G., 1997. Indole alkaloids from Aristotelia chilensis (Mol.). Stuntz Int. J. Pharm. 35, 215–217. 〈http://www.oie.int/en/animal-health-in-the-world/oie-listed-diseases-2017/〉.
Ji, D., Han, P., Zhang, J., Shao, Q., Liu, Y., Wang, L., Chen, G.F., 2009. Down-regulating effect of hepatitis B virus pre-S2 protein upon insulin receptor gene promoter. Zhonghua Yi Xue Za Zhi. 89, 3069–3073.
Keating, J.A., Bhattacharya, D., Lim, P.Y., Falk, S., Weisblum, B., Bernard, K.A., Sharma, M., Kuhn, R.J., Striker, R., 2013. West Nile virus methyltransferase domain interacts with protein kinase G. Virol. J. 22 (10), 242.
Kibenge, F.S.B., Lyaku, J.R., Rainnie, D., Hammell, K.L., 2000. Growth of infectious salmon anaemia virus in CHSE-214 cells and evidence for phenotypic differences between virus strains. J. Gen. Virol. 81, 143–150.
Kibenge, F.S., Kibenge, M.J., Groman, D., McGeachy, S., 2006. In vivo correlates of infectious salmon anemia virus pathogenesis in fish. J. Gen. Virol. 87, 2645–2652.
Korenaga, M., Wang, T., Li, Y., Showalter, L.A., Chan, T., Sun, J., Weinman, S.A., 2005. Hepatitis C virus core protein inhibits mitochondrial electron transport and increases reactive oxygen species (ROS) production. J. Biol. Chem. 280, 37481–37488.
Leal, E., Zarza, C., Tafalla, C., 2017. Effect of vitamin C on innate immune responses of rainbow trout (Oncorhynchus mykiss) leukocytes. Fish. Shellfish Immunol. 67, 179–188.
Lee, H.S., Lim, Y.S., Park, E.M., Baek, S.H., Hwang, S.B., 2014. SUMOylation of nonstructural 5A protein regulates hepatitis C virus replication. J. Viral Hepat. 21, 10.
Leitao, B.B., Jones, M.C., Brosens, J.J., 2011. The SUMO E3-ligase PIAS1 couples reactive oxygen species-dependent JNK activation to oxidative cell death. FASEB J. 25, 3416–3425.
Lin, X., Wang, R., Zou, W., Sun, X., Liu, X., Zhao, L., Wang, S., Jin, M., 2016. The influenza virus H5N1 infection can induce ROS production for viral replication and host cell death in A549 cells modulated by human Cu/Zn superoxide dismutase (SOD1) overexpression. Viruses 8, 8.
Manza, L.L., Codreanu, S.G., Stamer, S.L., Smith, D.L., Wells, K.S., Roberts, R.L., Liebler, D.C., 2004. Global shifts in protein sumoylation in response to electrophile and oxidative stress. Chem. Res Toxicol. 17, 1706–1715.
Mardones, F.O., Martinez-Lopez, B., Valdes-Donoso, P., Carpenter, T.E., Perez, A.M., 2014. The role of fish movements and the spread of infectious salmon anaemia virus (ISAV) in Chile, 2007–2009. Prev. Vet. Med. 114, 37–46.
Mattoscio, D., Segre, C.V., Chiocca, S., 2013. Viral manipulation of cellular protein conjugation pathways: the SUMO lesson. World J. Virol. 2, 79–90.
Meulmeester, E., Melchior, F., 2008. Cell biology: SUMO. Nature. 452 (7188), 709–711. https://doi.org/10.1038/452709a. (PubMed PMID: 18401402).
Mileva, M., 2016. Oxidative stress as a target for medication of influenza virus infection. Acta Microbiol. Bulg. 32, 3.
Miranda-Rottmann, S., Aspillaga, A., Prez, D., Vasquez, L., Martinez, A., Leighton, F., 2002. Juice and phenolic fractions of the berry Aristotelia chilensis inhibit LDL

oxidation in vitro and protect human endothelial cells against oxidative stress. J. Agric. Food Chem. 50, 7542–7547.
Muller, S., Berger, M., Lehembre, F., Seeler, J.S., Haupt, Y., Dejean, A., 2000. c-Jun and p53 activity is modulated by SUMO-1 modification. J. Biol. Chem. 275, 13321–13329.
Olavarría, V.H., Figueroa, J.E., Mulero, V., 2012. Prolactin-induced activation of phagocyte NADPH oxidase in the teleost fish gilthead seabream involves the phosphorylation of p47phox by protein kinase C. Dev. Comp. Immunol. 36, 216–221.
Olavarría, V.H., Gallardo, L., Figueroa, J.E., Mulero, V., 2010a. Lipopolysaccharide primes the respiratory burst of Atlantic salmon SHK-1 cells through protein kinase C-mediated phosphorylation of p47phox. Dev. Comp. Immunol. 34, 1242–1253.
Olavarría, V.H., Sepulcre, M.P., Figueroa, J.E., Mulero, V., 2010b. Prolactin-induced production of reactive oxygen species and IL-1β in leukocytes from the bony fish gilthead seabream involves Jak/Stat and NF-κB signaling pathways. J. Immunol. 185, 3873–3883.
Olavarría, V.H., Valdivia, S., Salas, B., Villalba, M., Sandoval, R., Oliva, H., Valdebenito, S., Yañez, A., 2015b. ISA virus regulates the generation of reactive oxygen species and p47phox expression in a p38 MAPK-dependent manner in Salmo salar. Mol. Immunol. 63, 227–234.
Olavarría, V.H., Recabarren, P., Fredericksen, F., Villalba, M., Yáñez, A., 2015a. ISAV infection promotes apoptosis of SHK-1 cells through a ROS/p38 MAPK/Bad signaling pathway. Mol. Immunol. 64, 1–8.
Ortega, J., Martin-Benito, J., Zurcher, T., 2000. Ultrastructural and functional analyses of recombinant influenza virus ribonucleoproteins suggest dimerization of nucleoprotein during virus amplification. J. Virol. 74, 156–163.
Pasquier, C., 1994. Oxidative Stress, Cell Activation and Viral Infection. BirkhäUser Verlag, Basel.
Prokudina, E.N., Semenova, N.P., Chumakov, V.M., 2005. Stability of intracellular influenza virus nucleocapsid protein oligomers. Arch. Virol. 150, 833–839.
Scherer, M., Reuter, N., Wagenknecht, N., Otto, V., Sticht, H., Stamminger, T., 2013. Small ubiquitin-related modifier (SUMO) pathway-mediated enhancement of human cytomegalovirus replication correlates with a recruitment of SUMO-1/3 proteins to viral replication compartments. J. Gen. Virol. 94, 1373–1384.
Schiøtz, B.L., Jørgensen, S.M., Rexroad, C., Gjøen, T., Krasnov, A., 2008. Transcriptomic analysis of responses to infectious salmon anemia virus infection in macrophage-like cells. Virus Res. 136, 65–74.
Shrivastava, V., Pekar, M., Grosser, E., Im, J., Vigodner, M., 2010. SUMO proteins are involved in the stress response during spermatogenesis and are localized to DNA double-strand breaks in germ cells. Reproduction 139, 999–1010.
Sies, H., 1997. Oxidative stress: oxidants and antioxidants. Exp. Physiol. 82, 291–295.
Snow, M., McKay, P., Macbeth, A.J.A., Black, J., Doig, F., Kerr, R., Cunningham, C.O., Nylund, A., Devold, M., 2006. Development, application and validation of a taqman® real-time RT-PCR assay for the detection of infectious salmon anaemia virus (ISAV) in Atlantic salmon (Salmo salar). In: Vannier, P., Espeseth, D. (Eds.), New Diagnostic Technology: Applications in Animal Health and Biologics Controls. Dev. Biol 126. Karger, Basel, pp. 133–145.
Takahashi, M., Higuchi, M., Makokha, G.N., Matsuki, H., Yoshita, M., Tanaka, Y., Fujii, M., 2013. HTLV-1 Tax oncoprotein stimulates ROS production and apoptosis in T cells by interacting with USP10. Blood 122, 715–725.
Truong, T.H., Carroll, K.S., 2012. Redox regulation of epidermal growth factor receptor signaling through cysteine oxidation. Biochemistry 51, 9954–9965.
Truong, T.H., Carroll, K.S., 2013. Redox regulation of protein kinases. Crit. Rev. Biochem. Mol. Biol. 48, 332–356.
Valenzuela-Miranda, D., Boltaña, S., Cabrejos, M.E., Yáñez, J.M., Gallardo-Escárate, C., 2015a. High-throughput transcriptome analysis of ISAV-infected Atlantic salmon Salmo salar unravels divergent immune responses associated to head-kidney, liver and gills tissues. Fish. Shellfish Immunol. 45, 367–377.
Valenzuela-Miranda, D., Cabrejos, M.E., Yañez, J.M., Gallardo-Escárate, C., 2015b. From the viral perspective: infectious salmon anemia virus (ISAV) transcriptome during the infective process in Atlantic salmon (Salmo salar). Mar. Genom. 20, 39–43.
Wang, C.-Y., Podolsky, R., She, J.-X., 2006. Genetic and functional evidence supporting SUMO4 as a type 1 diabetes susceptibility gene. Ann. N. Y. Acad. Sci. 1079, 257–267.
Wang, L., Banerjee, S., 2004. Differential PIAS3 expression in human malignancy. Oncol. Rep. 11, 1319–1324.
Watson, R.R., Schönlau, F., 2015. Nutraceutical and antioxidant effects of a delphinidin-rich maqui berry extract Delphinol®: a review. Minerva Cardioangiol. 63, 1–12 (Review).
Wilson, V.G., 2012. Sumoylation at the host-pathogen interface. Biomolecules 2, 203–227.
Wimmer, P., Schreiner, S., Dobner, T., 2012. Human pathogens and the host cell SUMOylation system. J. Virol. 86, 642–654.
Yang, P., Zhang, Y., Xu, J., Zhang, S., Yu, Q., Pang, J., Rao, X., Kuczma, M., Marrero, M.B., Fulton, D., Kraj, P., Su, Y., Wang, C.Y., 2013. SUMO1 regulates endothelial function by modulating the overall signals in favor of angiogenesis and homeostatic responses. Am. J. Transl. Res. 5, 427–440.
Yeh, E.T., 2009. SUMOylation and De-SUMOylation: wrestling with life's processes. J. Biol. Chem. 284, 8223–8227.
Youn, G.S., Cho, H., Kim, D., Choi, S.Y., Park, J., 2017. Crosstalk between HDAC6 and Nox2-based NADPH oxidase mediates HIV-1 Tat-induced pro-inflammatory responses in astrocytes. Redox Biol. 12, 978–986.